

# Thermoreversible gelation of organic liquids by arylcyclohexanol derivatives

## Synthesis and characterisation of the gels

Charles M. Garner,<sup>a</sup> Pierre Terech,<sup>b\*</sup> Jean-Jacques Allegraud,<sup>b</sup> Brian Mistrot,<sup>a</sup> Phuc Nguyen,<sup>a</sup> Arnaud de Geyer<sup>b</sup> and Daniel Rivera<sup>a</sup>

<sup>a</sup> Department of Chemistry, Baylor University, Waco, Texas 76798, USA

<sup>b</sup> Laboratoire Physico-Chimie Moléculaire, UMR 5819 CEA-CNRS-Université J. Fourier, Département de Recherche Fondamentale sur la Matière Condensée, C.E.A.-Grenoble, 17, rue des Martyrs, 38054 Grenoble Cedex 09, France

A variety of organic liquids can be immobilised using certain 4-*tert*-butyl-1-arylcylohexanol derivatives (BACOI). Only the isomers with axial aryl groups are active as gelling agents. The BACOI-hydrocarbon systems have been characterised with respect to their rheological properties under shear. The gels are viscoelastic solids with high elastic shear moduli ( $G' \approx 70350$  Pa at  $C \approx 2.2$  wt.% in dodecane) and high yield stresses ( $\sigma \approx 620$  Pa). A 3D network with high cohesive energy and long lifetimes of the related structures is in thermal equilibrium with the surrounding solution. Diffraction experiments have characterised the crystallinity of the gel networks made up of assemblies of bimolecular BACOI associations ( $d \approx 14.3$  Å). Xerogels exhibit a mesomorphic organisation with a 76 Å repeating unit. Phase diagrams have been determined as a function of the solvent and gelator types and the related thermodynamic parameters were deduced. IR spectroscopy has demonstrated that H-bonding is responsible for the aggregation of the BACOI molecules.

## 1 Introduction

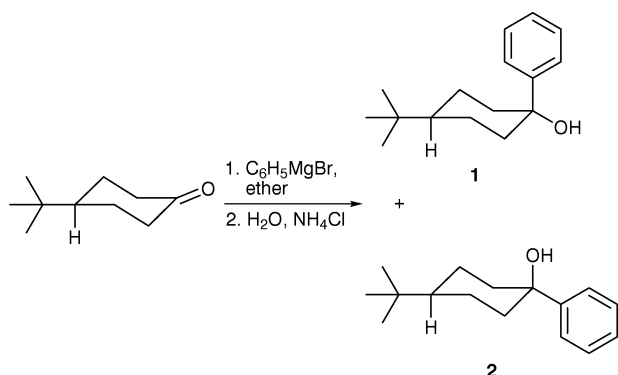
Gels are heterogeneous materials known for their spectacular ability to immobilise certain liquids. This property results from interfacial interactions between the liquid and a three-dimensional (3D) solid-like network mainly or totally constituted with the gelator itself. The thermal stability of the networks distinguishes the so-called 'chemical' gels, which are irreversible, from the 'physical' gels which exhibit a reversible liquid-to-gel phase transition. Physical gels exhibit a reversible melting transition from an elastic to a viscous behaviour at temperatures which can be currently below *ca.* 150 °C. A gel network can be pictured as a mesh of threads connected by nodes whose cohesive energy accounts for its thermal stability. The nodes or junction zones of physical gel networks involve weak forces, such as van der Waals interactions, which can be reinforced by electrostatic interactions, such as hydrogen bonding, electron transfer, ionic interaction, or weak organometallic coordination bonding.

Besides the well known class of synthetic or natural macromolecules<sup>1</sup> which form reversible gels<sup>2</sup> under appropriate concentration and solvent conditions, another important class of physical gels is constituted by special small molecules. Examples of low molecular weight compounds which can gel water<sup>3</sup> or organic liquids<sup>4</sup> are known. Such small gelator molecules have specific chemical functionalities responsible for the autoassociative behaviour operative in certain concentration-temperature-liquid conditions.

Gelator concentrations of at least *ca.* 0.5% are usually necessary to observe the hardening effect of organic liquids. Apolar organic liquids provide conditions for attenuated dipolar interactions between non-ionised species in the absence of the so-called hydrophobic interactions found with aqueous systems. Different types of small polarised molecules are available to form physical organogels. These include, for instance: fatty acids,<sup>5-7</sup> steroids,<sup>8</sup> aromatic gelators,<sup>9</sup> aromatic-steroid based gelators (for instance anthryl-<sup>10</sup> or

azobenzene-appended<sup>11</sup> cholesterol based gelators), long-chain alkylamide derivatives,<sup>12,13</sup> organometallic derivatives,<sup>14</sup> sorbitols,<sup>15</sup> bisurea derivatives<sup>16</sup> and acylated cellobioses,<sup>17</sup> *etc.* All these are non-ionic molecules which gel apolar hydrocarbons, unsaturated liquids, chlorinated solvents, nitriles and long-chain alcohols more or less selectively. A special class of ionic gelators (quaternary ammonium salts containing a cholestanyl group) is also known to form gels in alkanes, silicone oil, and alcohols, and one of them is even a gelator of propanol-water mixtures!<sup>18</sup> A large number of experimental observations<sup>4</sup> show both that gel formation and thermal stability of the related gels (as measured by their melting temperature, abbreviated as  $T_{GS}$ )<sup>12</sup> are dependent upon the type of gelled organic liquids. These phenomenological features are far from being understood. Dramatic variations are frequently<sup>19</sup> observed when minor changes are introduced in the chemical constitution (of either the gelator or the solvent) of the binary systems. At this stage, the combination of long aliphatic tails with potential site(s) for directional molecular connections are among the essential criteria for a molecule to be a gelator. These conditions illustrate the balance between attractive (*i.e.* specific bonding mechanisms) and repulsive conditions (fibre-fibre interactions) which make the occurrence of gelation a relatively rare phenomenon in which unidirectional (1D) crystallisation must occur rather than the ordinary tridimensional (3D) one.

The present paper reports the study of a family of 4-*tert*-butyl-1-arylcylohexanols, (BACOI, Schemes 1 and 2), which can form reversible organogels under surprising molecular configuration conditions. The BACOI structure consists of a phenyl group grafted to a 4-*tert*-butyl-1-cyclohexanol molecule: it appears that only the diastereoisomer with the aryl group in an axial configuration is an organogelator while the equatorial substitution does not lead to gels! BACOI gels also show a thermal stability clearly dependent upon the liquid type. The route for the synthesis of BACOI derivatives and the related sol-gel phase diagrams are determined and analysed.



**Scheme 1** BACOI derivatives: gelator **1** (*trans* isomer: phenyl group is axial); non-gelator **2** (*cis* isomer: aryl group is equatorial)

The mechanical characterisation of the gels is shown by rheology. IR and wide-angle X-ray scattering (WAXS) experiments provide some further clarification of the molecular aggregation mechanism.

## 2 Experimental

Except as noted, all reagents were used as received. 4-Fluorobromobenzene, pentafluorobromobenzene, magnesium, phenylmagnesium bromide and 4-*tert*-butylcyclohexanone were obtained from Aldrich Chemical Co. Anhydrous diethyl ether was obtained from Malinkrodt. Preparation and use of Grignard reagents were entirely under argon. Capillary gas chromatography was on an SE-54 column (30 m  $\times$  0.25 mm); the cleanliness of the injection port was important, because otherwise dehydration of these tertiary benzylic alcohols would occur to a significant extent (30% or more). With attention to this detail, dehydration was not important (<1%).

Proton NMR was at 360 MHz, and carbon NMR spectra were obtained at either 90 or 75 MHz and fluorine spectra were at 282 MHz.

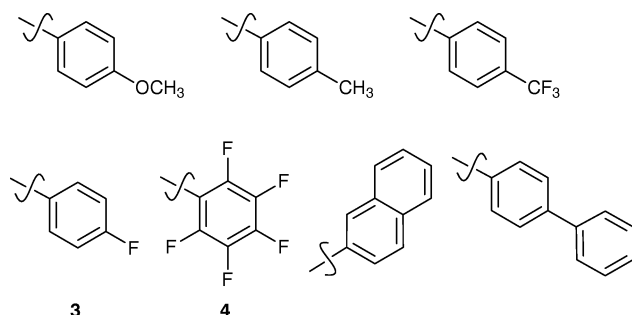
*trans*-4-*tert*-Butyl-1-phenylcyclohexanol (**1**) was prepared as previously reported;<sup>20</sup> a summary of a typical procedure follows. A solution of phenylmagnesium bromide (300 mmol) in 700 ml of anhydrous ether was cooled to  $-78^\circ\text{C}$  and treated slowly with a solution of 4-*tert*-butylcyclohexanone (41.6 g, 270 mmol) in 150 ml of ether. After warming slowly to room temperature, water (40 ml) was cautiously added with good stirring. Within a few minutes, a precipitate formed, leaving a clear organic phase. The organic phase was passed through a 2 cm pad of anhydrous sodium sulfate, and the precipitated magnesium salts were rinsed with additional ether. The filtrate was concentrated by rotary evaporation to yield first a gel, then, after prolonged exposure to a vacuum to constant weight, 61.5 g, of an off-white solid (crude yield  $\approx$  98%), which contained 62% *trans* (**1**) and 38% *cis* (**2**) isomers by capillary GC analysis. The isomers were easily separable by either column silica chromatography<sup>21</sup> or radial

chromatography (Harrison Research, Palo Alto, CA) using 100% dichloromethane as eluant, with the *trans* isomer eluting after the *cis* isomer.  $^1\text{H}$  NMR ( $\text{CDCl}_3$ ): 0.77 (s, 9H), 0.9–1.1 (m, 2H), 1.1–1.12 (m, 1H), 1.7–1.8 (m, 5H), 2.5–2.6 (m, 2H), 7.2–7.3 (m, 1H), 7.3–7.4 (m, 2H), 7.5–7.6 (m, 2H).  $^{13}\text{C}$  NMR ( $\text{CDCl}_3$ ): 24.9, 27.6, 32.2, 38.8, 47.8, 73.4, 126.4, 127.4, 128.5, 144.3.

*trans*-4-*tert*-Butyl-1-(4-fluorophenyl)cyclohexanol (**3**) was prepared as follows. Magnesium (1.48 g, 61 mmol) was suspended in anhydrous ether (20 ml) and 4-fluorobromobenzene (5.0 ml, 45.5 mmol) was added gradually over a 1 h period, during which time the initiation of the reaction was evident. After stirring for an additional 60 min, the Grignard reagent was cooled to  $-78^\circ\text{C}$  in a dry-ice–acetone bath, and a solution of 4-*tert*-butylcyclohexanone (5.6 g, 36.3 mmol) in 6 ml of ether was added dropwise. The reaction mixture was allowed to warm slowly to room temperature, then treated cautiously with 10%  $\text{NH}_4\text{Cl}$  solution (50 ml). An additional 50 ml of ether was added, and the organic phase was separated and dried over  $\text{MgSO}_4$ . Concentration by rotary evaporation yielded first a gel then, after prolonged exposure to a vacuum, an off-white solid, which was powdered with a mortar and pestle and dried under vacuum to constant weight. This gave 8.1 g (yield  $\approx$  90%) of a solid which by capillary GC analysis contained 64% *trans* (**3**) and 36% *cis* isomers. The isomers were easily separable by chromatography using dichloromethane as eluant (the *trans* isomer eluting after the *cis* isomer).  $^1\text{H}$  NMR ( $\text{CDCl}_3$ ): 0.8 (s, 9H), 0.9–1.1 (m, 2H), 1.1–1.2 (m, 1H), 1.6–1.8 (m, 4H), 2.0 (s, 1H), 2.4–2.5 (m, 2H), 7.0 (t, 2H,  $J = 8.8$ ), 7.49 (dd, 2H,  $J = 8.8$ , 5.4).  $^{13}\text{C}$  NMR ( $\text{CDCl}_3$ ): 24.9, 27.5, 32.2, 39.0, 47.7, 73.0, 115.1 (d,  $J = 21$ ), 128.2 (d,  $J = 7$ ), 140.1 (d,  $J = 4$ ), 161.4 (d,  $J = 244$ ).  $^{19}\text{F}$  NMR ( $\text{CDCl}_3$ ):  $-115.8$  (tt,  $J = 8.8$ , 5.4).

*trans*-4-*tert*-Butyl-1-(pentafluorophenyl)cyclohexanol (**4**) was prepared as follows. Magnesium (1.31 g, 54 mmol) was suspended in anhydrous ether (10 ml) and pentafluorobenzene (5.0 ml, 40.1 mmol) was added in small amounts until reaction had commenced, with the remainder added gradually over a 2 h period. After stirring for an additional 2 h, the Grignard reagent was diluted with additional ether (20 ml). A solution of 4-*tert*-butylcyclohexanone (4.9 g, 32 mmol) in 20 ml of ether was added dropwise to the Grignard reagent with the flask immersed in a room temperature water bath. The reaction mixture was stirred at room temperature for 1 h, then treated cautiously with 10%  $\text{NH}_4\text{Cl}$  solution (100 ml). The aqueous–organic mixture was filtered through a 2 cm pad of silica gel, and rinsed with an additional 50 ml of ether. The brown organic phase was separated, washed once with saturated sodium chloride solution and dried over  $\text{MgSO}_4$ . Concentration by rotary evaporation yielded first a gel then, after prolonged exposure to a vacuum, a tan solid. This material could not reproducibly be analysed by capillary GC because partial decomposition to 4-*tert*-butylcyclohexanone was observed to occur in the GC injection port and was sensitive to the injection port temperature. However, the *cis* and *trans* isomers were easily separable by either radial or column chromatography using 100% as eluant, with the *trans* isomer **4** eluting after the *cis* isomer.  $^1\text{H}$  NMR ( $\text{CDCl}_3$ ): 0.82 (s, 9H), 0.9–1.2 (m, 3H), 1.55–1.7 (m, 2H), 1.75–1.9 (m, 2H), 2.45 (s, 1H), 2.78 (br d, 2H,  $J = 13.6$ ).  $^{13}\text{C}$  NMR ( $\text{CDCl}_3$ ): 25.1, 27.5, 32.2, 40.0, 47.2, 76.0, 118.1 (br s), 137.9 (br d,  $J = 248$ ), 140.2 (br d,  $J = 254$ ), 146.1 (br d,  $J = 250$ ).  $^{19}\text{F}$  NMR ( $\text{CDCl}_3$ ):  $-138.2$  (m, 2F),  $-155.9$  (tt, 1F,  $J = 21$ , 4),  $-162.3$  (m, 2F).

BACOI is a solid of low solubility in non-polar solvents (cyclohexane, benzene, carbon tetrachloride, etc.). However, with warming, the solid dissolves, and upon subsequent cooling, a gel results. The turbid appearance of concentrated gels was sensitive to the solvent type and concentration. Toluene or benzene gels appeared transparent while concentrated gels in heptane or dodecane were turbid. The gel-like



**Scheme 2** Substituted aryl groups incorporated in 1-aryl-4-*tert*-butylcyclohexanols; only the ring-fluorinated compounds **3** and **4** are organogelators

samples were colloidal in nature as demonstrated by the visible trace of an incident laser beam in the gel. Gels were often stable for months before a solid liquid phase separation process was observed for some of them (*i.e.* in heptane).

Rheology experiments, conducted in the linear regime of deformations, used a Haake RS100 stress rheometer in a frequency range 0.001–61 Hz. A plate–plate geometry was used (20 mm diameter, 0.25 mm gap) with serrated surfaces so as to prevent sliding due to the liquid film expelled by certain dilute samples. In addition to the choice of an organic liquid with a high boiling point (dodecane:  $T_b = 216^\circ\text{C}$ ), a special device was used to limit any solvent evaporation. The temperature was regulated with an accuracy better than  $0.1^\circ\text{C}$ . The gel was allowed to form between the two plates of the rheometer after preliminary introduction of the heated solution. After an equilibration time of *ca.* 1 h of the gelling system, the measurements of the rheological behaviour were started.

To determine the gel melting temperatures,  $T_{GS}$ , the gels were prepared in 5 mm tubes closed at one end and capped at the other with a septum. A small Teflon-coated magnetic stir bar was included. The dropping of the stir bar during the very slow temperature ramp (to which the gel is submitted) indicates the gel melting temperature. For each solvent, the measurement was repeated with three separate samples at each concentration, and was typically reproducible to  $\pm 0.5^\circ\text{C}$ .

WAXS experiments were performed with an Elliot GX 20 rotary anode generator, using the Cu  $K\alpha$  radiation from a copper anode. X-Rays from a fine focus source ( $100\ \mu\text{m} \times 100\ \mu\text{m}$ ) were  $K\alpha/K\beta$  filtered ( $\lambda = 1.54\ \text{\AA}$ ) and 2D focused by using the total reflection from two orthogonally curved mirrors (Ni-coated glass flats). A linear gas-filled detector (4000 channels) was used at a sample-detector distance  $l = 193\ \text{mm}$  and the angular range was  $0.9^\circ < 2\theta < 10.4^\circ$  [corresponding to a transfer momentum range  $Q = 4\pi/\lambda(\sin \theta)$   $0.0634 < Q < 0.74\ \text{\AA}^{-1}$ ]. Experimental intensities (in arbitrary units) were normalised to the detector response by dividing spectra by a flat fluorescence signal provided by a 25  $\mu\text{m}$  thick cobalt foil.

IR studies used a solution ( $C = 4\ \text{wt.}\%$ ) of gelling agent **1** in  $\text{CCl}_4$  transferred warm to a variable-temperature IR cell (Wilma Glass Co.) with *ca.* 1 mm pathlength in a Perkin Elmer 1600 FTIR spectrometer. UV absorption spectra were obtained (not shown) from a Beckman spectrometer, but failed to show significant differences between the gelled and liquid states.

### 3 Results

In the course of synthesising a series of substituted cyclohexanones, new organic gelling agents were discovered. The arylcyclohexanol gelators are 4-*tert*-butyl-1-arylcylohexanol derivatives (**1** and **2**, abbreviated to BACOI), which are prepared as shown in Scheme 1. The gelation phenomenon was mentioned<sup>20</sup> many years ago but not studied. The *trans* isomer **1** predominates in an approximately 65 : 35 ratio, depending on the reaction temperature. Interestingly, only the *trans* diastereoisomer with the axial aryl group (**1**), which is also the more polar, exhibits a gelation ability. The gel is stable to the presence of additional hydrocarbon solvents or water and liquefies with a well defined ‘melting point’  $T_{GS}$  upon heating.  $T_{GS}$  depends both on the polarity and type of organic liquid and on the concentration of the gelling agent: less polar solvents are immobilised at lower concentrations, and higher concentrations of **1** always result in higher melting points. For example, heptane is immobilised at room temperature with only 0.7 wt.% of the gelling agent. Fig. 1A shows the relationship between the melting points of several gelled liquids and the concentrations of the gelator. The process is completely reversible with warming, provided crys-

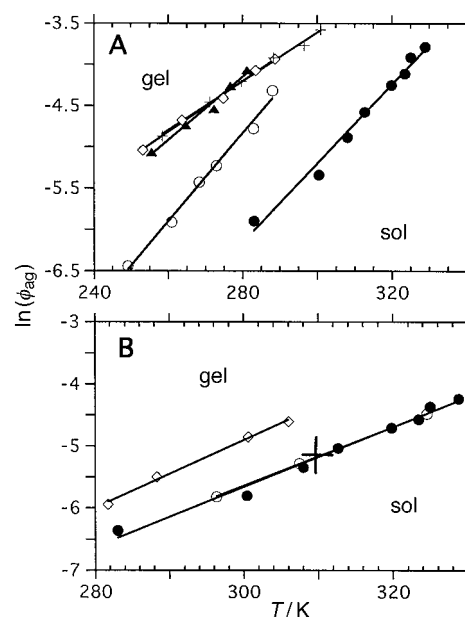


**Fig. 1** Concentration–temperature phase diagrams  $\ln(\phi_{ag})$  vs.  $T$  of BACOI (compound **1**) and fluorinated derivative organogels. Each continuous line separates the fluid solution domain (high temperature) from the solid-like gel domain (low temperature). A, Solvent type dependence;  $\bullet$  = heptane,  $\circ$  = toluene,  $\diamond$  = ether,  $\blacktriangle$  = dichloromethane,  $+$  = ethyl acetate. B, Comparison of BACOI gelling agents in heptane (numbers refer to structures as in Scheme 1 and 2);  $\circ$  = (**3**) *p*-fluorophenyl,  $\bullet$  = phenyl (**1**),  $\diamond$  = (**4**) pentafluorophenyl. The bold cross ( $+$ ) indicates the melting point ( $T = 308.8\ \text{K}$ ) of a gel made up of a mixture ( $C = 1.375\ \text{wt.}\%$ ) of the gelling isomer (**1**, 51%) and non-gelling isomer (**2**, 49%).

tallisation does not intervene. The hardening of organic liquids is not affected by the presence of the inactive isomer in the system (Fig. 1B). The gelator can ‘crystallise’ to a fibrous solid if a germination process is induced by either seeding, evaporation of the solvent or possibly by mechanical agitation. However, crystallisation is easily avoided, particularly in low volatility solvents (*e.g.* mineral oil). Even when crystallisation is induced, it is exceedingly slow in the gelled state and generally requires gentle warming. Among the liquids studied, only methanol and ethanol could not be gelled with BACOI since crystallisation occurred immediately.

In order to foster the understanding of the mechanisms that underlie the molecular aggregation/gelation phenomena, we investigated the structural variations which could be accomplished without losing the gelation properties associated with compound **1**. To this purpose, a variety of derivatives with substituted aromatic rings were prepared (Scheme 2). The BACOI system proved to be quite sensitive to such structural variations: of all the derivatives mentioned in Scheme 2, only the ring-fluorinated compounds **3** and **4** (diastereoisomers having an axial aryl group) showed a gelation ability. It was impossible to obtain any of the ‘gel active’ diastereoisomers as single crystals suitable for X-ray analysis; ‘crystallisation’ results only in very fibrous solids. However, the diastereoisomers with an equatorial aryl group are crystalline, and the stereochemistry was confirmed by X-ray analysis of the *cis-p*-fluoro derivative. Fig. 1B shows the phase diagrams for the BACOI derivatives **1**, **3** and **4** in heptane.

A rheological characterisation of the BACOI–dodecane system is shown in Fig. 2 and 3. Fig. 2A displays the viscous ( $G'$ ) and elastic ( $G''$ ) responses of a gel ( $C = 2.2\ \text{wt.}\%$ ) submitted to an oscillatory stress with constant amplitude ( $\sigma = 10\ \text{Pa}$ ) in the linear regime of deformations. The rheological parameters are calculated<sup>22</sup> respectively from the phase lag between the applied shear stress and the related flow and from the ratio of the amplitudes of the imposed oscillation to the response of the gel.  $G'$ ,  $G''$ ,  $\eta^*$  (complex viscosity) are linked

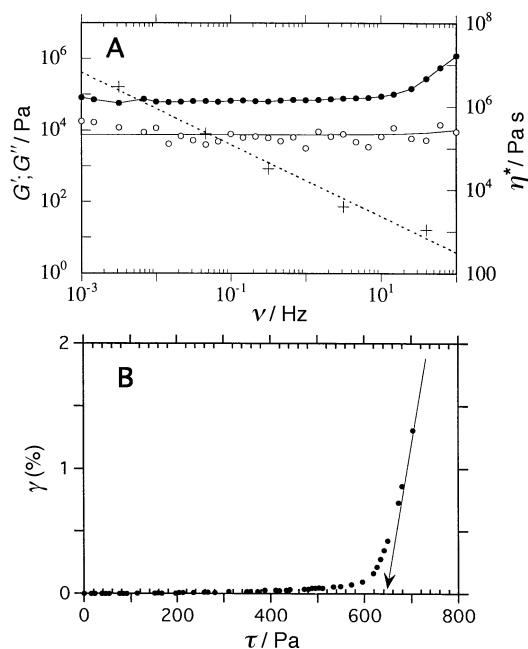


**Fig. 2** Rheology of the BACOI (I)-dodecane system ( $C = 2.2$  wt.%). A, Dynamic experiment: a constant oscillatory stress ( $\sigma = 10$  Pa,  $10^{-3} < \nu < 61$  Hz) is applied to the organogel in the linear regime of deformations at  $T = 20^\circ\text{C}$ . The elastic modulus  $G'$  (●) and the loss modulus  $G''$  (○) are shown. B, Flow experiment: the gel sandwich is submitted to a constantly increasing stress  $\sigma$  ( $d\sigma/dt \approx 0.15$  Pa  $\text{s}^{-1}$ ), while its deformation  $\gamma$  (proportional to the angular displacement) is measured. The gel starts to flow at  $\sigma^* \approx 620$  Pa.

together as follows  $|\eta^*(\omega)| = [G'^2(\omega) + G''^2(\omega)]^{1/2}/\omega$  where  $\omega$  is the angular frequency ( $\omega = 2\pi\nu$ ). At this concentration, the elastic shear modulus  $G'$  (70350 Pa), at  $\nu = 1$  Hz, is much greater than  $G''$  (3202 Pa) and about constant over at least 4 frequency decades in the  $10^{-3}$ –10 Hz range. Fig. 2B shows a flow experiment with a BACOI-dodecane system at  $C = 2.2$  wt.%: no significant flow occurs for stresses below a limiting stress  $\sigma^* \approx 620$  Pa. Fig. 3 illustrates the thermal reversibility of the sol to gel and gel to sol phase transitions as probed by rheology. Related values of the transition temperatures,  $T_{\text{SG}} = 28.7^\circ\text{C}$  and  $T_{\text{GS}} = 45.7^\circ\text{C}$ , can be estimated and a large hysteresis effect is clearly observed.

Wide-angle X-ray diffraction experiments (WAXS) were employed to characterise the crystallinity of the systems. Fig. 4 presents the diffraction patterns of a BACOI crystalline powder (curve 1) used to prepare the gels, a xerogel (curve 2) obtained from a cyclohexane gel and a gel in dodecane at  $C = 10$  wt.% (curve 3).

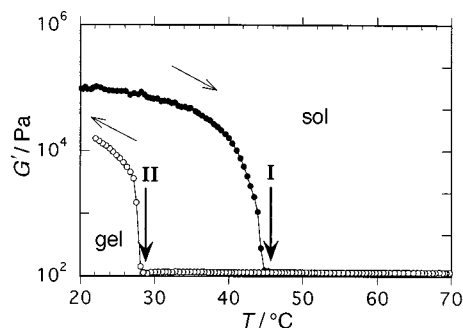


**Fig. 3** Thermal reversibility of the sol to gel phase transition of a BACOI-dodecane system ( $C = 2.2$  wt.%). The elastic modulus  $G'$  is recorded in an oscillatory experiment ( $\sigma = 10$  Pa and  $\nu = 1$  Hz) while the temperature  $T$  is varied ( $dT/dt \approx 0.83^\circ\text{C min}^{-1}$ ) in the range  $20$ – $70^\circ\text{C}$ . Bold vertical arrows are for the transitions: melting (●), (I,  $T_{\text{GS}} \approx 45.7^\circ\text{C}$ ) and subsequent re-gelation on cooling (○), (II,  $T_{\text{SG}} \approx 28.7^\circ\text{C}$ ). The rheograms delimit the gel and sol domain.

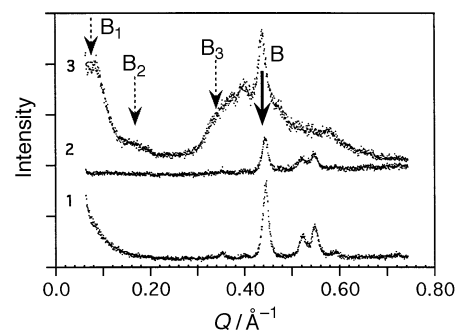


**Fig. 4** WAXS patterns of BACOI crystalline powder (curve 1), a gel in dodecane (curve 2) at  $C = 10.0$  wt.%, a xerogel (curve 3) obtained from a cyclohexane gel. The bold arrow points at  $Q \approx 0.44 \text{ \AA}^{-1}$  corresponding to the bimolecular distance  $ca. 14.3 \text{ \AA}$ . For the xerogel pattern (curve 3), dotted arrows indicate three additional diffraction features at  $Q \approx 0.0825 \text{ \AA}^{-1}$  ( $B_1$ ),  $Q \approx 0.165 \text{ \AA}^{-1}$  ( $B_2$ ) and  $Q \approx 0.44 \text{ \AA}^{-1}$  ( $B_3$ ).

The structural investigation was pursued towards smaller length-scales using the IR and UV spectroscopies. Since BACOI is an hydroxylated compound (Scheme 1), it was reasonable to expect the participation of H-bonds in the mechanism of molecular aggregation leading to the gels. In the O–H stretching region (Fig. 5), a gel at  $C = 4$  wt.% in  $\text{CCl}_4$  exhibited three broad absorptions ( $3189$ ,  $3280$ ,  $3450 \text{ cm}^{-1}$ ; intensity  $I$  estimated by the area of the absorption bands is  $ca. 80\%$  of total OH bands) and a narrow peak ( $3603 \text{ cm}^{-1}$ ,  $I \approx 20\%$ ). Upon warming above the melting point, only the  $3450$  and  $3603 \text{ cm}^{-1}$  absorptions remained, with the latter increasing significantly ( $I \approx 50\%$  at  $80^\circ\text{C}$ ) as the temperature increased.

#### 4 Analysis and Discussion

The solid-like consistency of the BACOI-organic liquid systems is typical of a self-supported gel. The recognition of

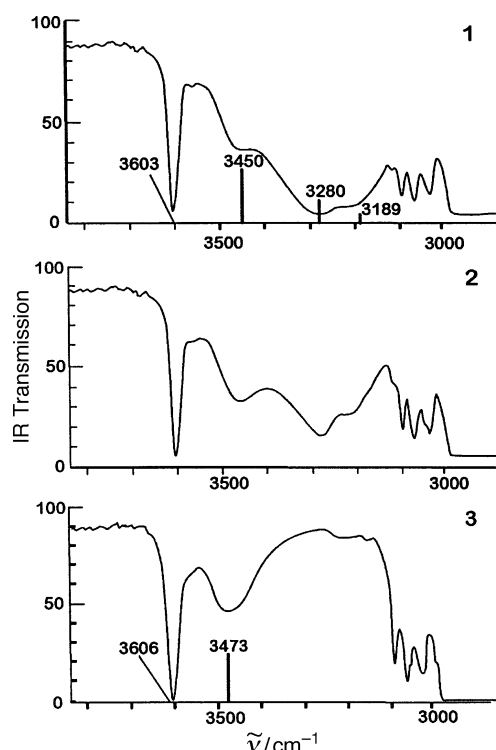


**Fig. 5** IR spectra of a BACOI organogel in  $\text{CCl}_4$  ( $C = 4$  wt.%) at increasing temperatures. 1:  $T = 29.0^\circ\text{C}$  (gel phase); 2:  $T = 40.0^\circ\text{C}$ ; 3:  $T = 80.0^\circ\text{C}$  (liquid phase). The absorption in the  $3000 \text{ cm}^{-1}$  region is due to CH stretching vibrations.



the gel state can be formalised by taking advantage of its rheological properties:<sup>23</sup> the storage modulus  $G'(\nu)$  exhibits a pronounced plateau extending to times of at least 1000 s and which is significantly greater than the loss modulus  $G''(\nu)$ . The large  $G'$  value (70350 Pa at  $\nu = 1$  Hz and  $C = 2.2$  wt.%) can be compared to common values observed for molecular gels with crystalline 3D networks (*i.e.* made of rigid fibres fused into crystalline microdomains). For instance, the 12-hydroxystearic acid–dodecane gel is a solid-like crystalline gel with a high elasticity  $G' \approx 8220$  Pa (while  $G'' \approx 560$  Pa) at  $C = 1.27$  wt.%. In this case, the high value of the storage modulus was interpreted as resulting from the existence of crystalline microdomains<sup>7</sup> whose monoclinic symmetry was sensitive to the solvent type. It has been shown<sup>24</sup> that with idealised networks in which frozen crosslinks are permanent and rigid (*i.e.* not freely hinged) and chains are straight, the elastic modulus scales as the second power of the volume fraction (*i.e.*  $G' \approx \phi^2$ ). Taking into account the concentration difference, the value  $G' = 70350$  Pa for the BACOI system must be compared to the value  $G' \approx 24666$  Pa of the fatty acid ‘reference system’. A significant difference exists which may reveal the specificity of the BACOI molecular aggregation mechanism in relation to the bending energy of the constitutive rigid rods. The large values of the storage elastic modulus and yield stress indicate that interactions between the BACOI colloidal aggregates are energetic associations able to form long-lived rigid networks. The present rheology experiments qualify the BACOI–hydrocarbon systems as viscoelastic solid-like gels.

Gelation of organic solutions by BACOI is a thermoreversible transition and exhibits a large hysteresis effect (*ca.* 20 °C) as shown in Fig. 3. Hysteresis is a common feature with the class of low-mass organogels. Close analogies exist between gelation and the crystallisation behaviour of supersaturated solutions. Crystallisation results from two simultaneous processes, the formation of nuclei of the new phase and the growth of crystals which is frequently a first-order process, specially when involving hydrogen bond connections. The germination reactions of the sol to gel phase transition can be kinetically the limiting steps compared to the speed of the imposed temperature sweep experiment as revealed by the large temperature difference observed with Fig. 3 (*ca.* 17 °C).

The shearing stress can also affect the aggregation process (*i.e.* through orientational effects) as suggested by the incomplete elastic recovering observed at  $T = 20$  °C during the sol to gel transition of Fig. 3 (Cycle II, vertical axis).

The phase diagrams of the BACOI–hydrocarbon systems are shown in Fig. 1 in a specific representation  $\ln(\phi_{ag})$  *vs.*  $T$  ( $\phi_{ag}$  being the unit mole fraction of gelator at temperature  $T$ ). The specific representation is convenient when thermodynamic parameters are to be determined since they are proportional to the slope  $\partial \ln \phi_{ag} / \partial T$  [see eqn. (1)]. It also facilitates the distinction of different groups of auto-associative systems according to their enthalpic values. Thus, three groups of liquids can be distinguished: heptane, toluene and a group with ether, ethyl acetate and dichloromethane. Heptane gels have a higher melting point while gels with larger alkanes exhibit increasingly higher melting points at a fixed concentration (Fig. 6). Thermodynamic parameters of the aggregate formation can be evaluated using eqn. (1).<sup>12,22,25</sup>  $T$  is the absolute temperature,  $\Delta G_{ag}^\circ$  is the standard free energy,  $\Delta H_{ag}^\circ$  is the standard free enthalpy and  $\Delta S_{ag}^\circ$  is the entropy of formation of the aggregates through a phase separation process. Interestingly, the growing aggregates of this class of low-mass gelators have been shown to be fibres with polydisperse lengths as they result from thermal equilibria while their cross-sections can be frequently monodisperse (with finite cross-sectional aggregation numbers).<sup>7</sup>

$$\Delta G_{ag}^\circ = RT \ln(\phi_{ag}) \quad (1a)$$

$$\Delta H_{ag}^\circ = -RT^2 \left( \frac{\partial \ln(\phi_{ag})}{\partial T} \right) \quad (1b)$$

$$\Delta S_{ag}^\circ = -R \ln(\phi_{ag}) - RT \left( \frac{\partial \ln(\phi_{ag})}{\partial T} \right) \quad (1c)$$

The thermoreversible gelation transition occurs during the course of the molecular aggregation reactions forming fibrillar structures. The thermodynamic parameters which describe the aggregation also describe the physical gelation from small molecules. Tables 1 and 2 show that the enthalpic contribution compensates for the entropic change in all investigated situations (liquid or gelator changes). The standard enthalpy

**Table 1** Gel/sol phase diagrams [ $\ln(\phi_{ag})$  *vs.*  $T$ ] of BACOI in hydrocarbons

solvent	$\frac{\partial \ln(\phi_{ag})^{a,b}}{\partial T}$	$\Delta H_m^\circ / \text{kJ mol}^{-1}$	$\ln(\phi_{ag})^a$	$\Delta S_m^\circ / \text{J K}^{-1} \text{mol}^{-1}$
heptane	0.048057	−35.6	−5.29	−75.5
toluene	0.053197	−39.7	−3.88	−100.2
ether	0.031005	−23.0	−3.64	−46.8
dichloromethane	0.038277	−28.5	−3.46	−66.5
ethyl acetate	0.029773	−22.2	−3.67	−43.5

<sup>a</sup>  $\phi_{ag}$  is the unit mol fraction;  $T$  is in K. <sup>b</sup>  $\partial \ln(\phi_{ag}) / \partial T$  is the slope of the phase diagram ( $\text{K}^{-1}$ ). <sup>c</sup>  $\Delta H_m^\circ$  is the standard enthalpy at 20 °C for the melting transition of the gels. <sup>d</sup>  $\Delta S_m^\circ$  is the standard entropy at 20 °C for the melting transition of the gels.

**Table 2** Gel/sol phase diagrams [ $\ln(\phi_{ag})$  *vs.*  $T$ ] of 1, 3 and 4 derivatives in heptane

derivative <sup>a</sup>	$\frac{\partial \ln(\phi_{ag})^{b,c}}{\partial T}$	$\Delta H_m^\circ / \text{kJ mol}^{-1}$	$\ln(\phi_{ag})^b$	$\Delta S_m^\circ / \text{J K}^{-1} \text{mol}^{-1}$
1	0.048221	−36.0	−5.75	−72.0
3	0.047386	−35.2	−5.73	−70.3
4	0.0546	−40.6	−5.01	−94.2

<sup>a</sup> Numbers refer to the formulae in Schemes 1 and 2. <sup>b</sup>  $\phi_{ag}$  is the volume fraction;  $T$  is in K. <sup>c</sup>  $\partial \ln(\phi_{ag}) / \partial T$  is the slope of the phase diagram ( $\text{K}^{-1}$ ). <sup>d</sup>  $\Delta H_m^\circ$  is the standard enthalpy at 20 °C for the melting transition of the gels. <sup>e</sup>  $\Delta S_m^\circ$  is the standard entropy at 20 °C for the melting transition of the gels.

of melting is dependent upon the liquid type which might reveal a sensitivity of the BACOI structures with the liquid type in a similar way to the polytypism phenomenon encountered with long-chain derivatives<sup>26</sup> such as the mentioned 'reference' fatty acid (*vide supra*). Due to the chemical constitution of BACOI, it is reasonable to expect the participation of hydroxy groups in the aggregation mechanism (*vide infra*). A typical value for hydrogen bonding is of the order of  $\Delta H \approx 16\text{--}21 \text{ kJ mol}^{-1}$ <sup>27</sup> which suggests that the interaction which makes  $\Delta H$  negative might arise not only from hydrogen bonding between the hydroxy groups (a contribution from dipolar interactions between the aromatic polarised rings and van der Waals interactions may also be required).

A comparison of the phase diagrams for the three gelators **1**, **3** and **4** (Fig. 1B and Table 2) shows that the standard free energy is comparable and suggests that the mechanisms of aggregation and the related degrees of molecular ordering within the aggregates are similar. WAXS experiments (Fig. 4) show that the molecular structure of the BACOI crystal and xerogel present both similarities and differences. An intense and narrow Bragg peak at  $Q \approx 0.44 \text{ \AA}^{-1}$  is common to the two solids (curves 1 and 3) and can also be distinguished with the organogel in dodecane (curve 2). The corresponding reticular distance is *ca.*  $14.3 \text{ \AA}$  which is approximately the BACOI bimolecular length ( $2 \times 6.6 \text{ \AA}$ ). It can be concluded that the BACOI networks include crystalline-like heterogeneities made up of organised associations of bimolecules. These microdomains can be assimilated with the junction zones of the BACOI elastic networks. It is remarkable to observe that most of the typical diffraction features observable on the pattern of the crystalline solid (curve 1) can be distinguished in the pattern of the dodecane gel (curve 2). For instance, two additional intense peaks of the crystalline powder at  $Q \approx 0.521 \text{ \AA}^{-1}$  and  $Q \approx 0.546 \text{ \AA}^{-1}$  are also emerging in the gel pattern and appear broadened. BACOI colloids and the crystalline powder are constituted of bimolecular associations. The xerogel is further organised over much larger distances as characterised by the existence of peaks  $B_1$  ( $Q \approx 0.0825 \text{ \AA}^{-1}$ ),  $B_2$  (broad,  $Q \approx 0.165 \text{ \AA}^{-1}$ ) and  $B_3$  (very broad,  $0.3 < Q < 0.4 \text{ \AA}^{-1}$ ). A repeating distance  $d = 2\pi/0.0825 \approx 76 \text{ \AA}$  is typical of the mesomorphic organisation of the xerogel. The xerogel results from the collapse and merging process of the native solvated colloids (by solvent evaporation) which can form locally oriented bundles of colloids (most frequently fibres). The distance  $76 \text{ \AA}$  characterises such basic colloids further ordered in a symmetry revealed by  $B_2$  and  $B_3$  peaks over relatively small correlation distances (as suggested by the width of peaks). Due to the broadness of the  $B_2$  and  $B_3$  peaks, a clear identification of the symmetry of the xerogel mesomorphic organisation cannot be obtained. Assuming that the typical distance  $d = 76 \text{ \AA}$  is the diameter of fibrillar colloids, the cross-sectional molecular organisation appears to be complex since no simple relation appears to link the bimolecular length to  $d$ . Further experiments are required to characterise the morphology of the BACOI colloids and will be presented in a forthcoming paper.<sup>28</sup> The increase of  $T_{GS}$  with the chain length of the gelled alkanic liquid (Fig. 6) suggests that crystallinity and melting temperatures of BACOI gels can be correlated.

IR spectroscopy shows (Fig. 5) that H-bonding is a major mechanism for the aggregation of BACOI molecules to the colloids of the gels. The O—H stretching vibration at  $3603 \text{ cm}^{-1}$  (narrow) is due to the unaggregated BACOI species while the two bands at  $3189$  and  $3280 \text{ cm}^{-1}$  (broad) correspond to the stretching of O—H bonded links. An increase of temperature (in the sol domain) disorganises the BACOI colloids made up with associated bimolecules. As a consequence, the fraction of isolated gelators is increased (enhancement of the band at  $3603 \text{ cm}^{-1}$ ) as well as the fraction of small  $n$ -mers (*i.e.* dimers) to which corresponds the increase of the band at

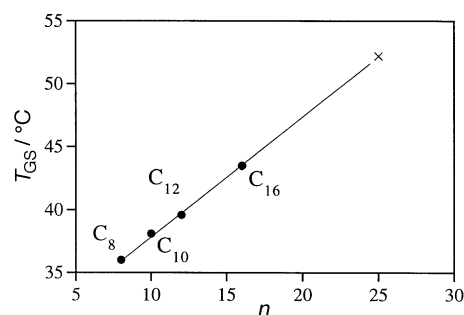


**Fig. 6** Melting temperatures  $T_{GS}$  of gels ( $C = 1 \text{ wt.}\%$ ) of straight-chain hydrocarbons as a function of carbon number  $n$  in  $n$ -alkanes. Alkanes ( $C_nH_{2n+2}$ ) are indicated by  $C_n$  labels. The value for a mineral oil (x) is forced to lie on the best straight line ( $0.926n + 28.6$ ) by assuming 25 carbons.

$3450 \text{ cm}^{-1}$ . Simultaneously, the amplitudes of the bands typical of the large aggregates are decreased ( $3280, 3189 \text{ cm}^{-1}$  bands). The band at  $3450 \text{ cm}^{-1}$  keeps a significant amplitude even at high temperatures in the sol domain which is consistent with the existence of strong bimolecular associations which are the building units of the BACOI colloids in the gel phase. The present phenomenology has already been observed with different hydroxylated auto-associative molecules.<sup>5,29</sup> The enthalpy values of Tables 1 and 2 indicate that H-bonding is not a unique driving force for the BACOI aggregation reactions. Attractive interactions, such as van der Waals and dipolar interactions involving polarised BACOI molecules with  $\sigma$  and  $\pi$  electronic densities, are probably additional components for the free energy. A 3D network of crystalline-like colloids is formed during the sol to gel phase transition and exhibits both a lifetime and an elastic shear modulus revealing the existence of strong interactions. The solid-like network is in thermal equilibrium (Fig. 1) with the liquid surrounding medium which contains 'isolated' BACOI species or small non-interconnected aggregates (sol part of the phase diagram). The thermal hysteresis and the phase separation behaviours are phenomena which suggest that nucleation and crystal growth reactions are important parameters for the growth and subsequent topology of the interconnected network of colloidal crystalline-like aggregates. It is interesting to note that hydrogen bonding is the most common aggregation mechanism encountered with hydroxylated or amino organogelators. Some non-hydrogen bonding organogelators are also known to develop fibres through stacking mechanisms between polarised aromatic molecules<sup>9</sup> or organometallic coordinated species.<sup>14</sup> Different systems have already shown an aggregation ability and/or structures of the resulting aggregates affected by the spatial configuration at the major site for molecular aggregation of the gelator. As an example, azobenzene organogelators develop a marked dependency of their gelation behaviour upon the configuration at the C3 of the steroid moiety.<sup>11</sup> A second example is that of organogels made from substituted octadecanoic acids which show relationships between the optical activity of the gelator and the helicity of the fibre-like aggregates of the gels.<sup>30</sup> In organic liquids, the influence of the molecular configuration of the gelator upon the aggregation/gelation capacity is usually not as important<sup>7</sup> as it can be with aqueous analogues, where racemic gelators are known to produce gels with restricted lifetimes as a consequence of the so-called 'chiral bilayer effect'.<sup>31</sup> Here, with BACOI derivatives, the configuration at the carbon bearing the hydroxy group remarkably determines the aggregation/gelation behaviour. Incidentally, a close derivative, 4-*tert*-butyl-1-phenylcyclohexane,<sup>20</sup> has shown that the phenyl group prefers the equatorial position of the cyclohexane ring (*i.e.* the *trans* conformation is more stable than the *cis* one by  $\Delta H = 15.0 \text{ kJ mol}^{-1}$ ). If such a situation is preserved in BACOI diastereoisomers (**1** and **2**),

it may account for the metastability of **1** organogels despite the fact that the conversion of **1** to **2** remains impossible.

In conclusion, the thermal and mechanical characterisations of BACOI organogels have shown that a solid-like network was formed by bimolecular associations. Crystalline microdomains are acting as elastically active junction zones of the gel networks. The related xerogels exhibit a long-range mesomorphic organisation with a characteristic repeating unit of 76 Å size. H-bonding is a major mechanism in the BACOI gelation phenomenon which form colloidal structures through solvent-dependent dipolar interactions.

## References

- 1 P. S. Russo, in *ACS Symp. Ser.*, 1987, vol. 350, ch. 9, ACS, Washington, DC.
- 2 P. H. Hermans, in *Colloid Science, Reversible Systems, II*, Elsevier, Amsterdam, 1969.
- 3 B. Pfannemüller and W. Welte, *Chem. Phys. Lipids*, 1985, **37**, 227.
- 4 P. Terech and R. G. Weiss, *Chem. Rev.*, 1997, **97**, 3133.
- 5 T. Tachibana, T. Mori and K. Hori, *Bull. Chem. Soc. Jpn.*, 1980, **53**, 1714.
- 6 T. Tachibana, T. Mori and K. Hori, *Bull. Chem. Soc. Jpn.*, 1981, **54**, 73.
- 7 P. Terech, V. Rodriguez, J. D. Barnes and G. B. McKenna, *Langmuir*, 1994, **10**, 3406.
- 8 R. H. Wade, P. Terech, E. A. Hewat, R. Ramasseul and F. Volino, *J. Colloid Interface Sci.*, 1986, **114**, 442.
- 9 T. Brotin, R. Utermöhlen, F. Fages, H. Bouas-Laurent and J. P. Desvergne, *J. Chem. Soc., Chem. Commun.*, 1991, 416.
- 10 Y.-c. Lin, B. Kachar and R. G. Weiss, *J. Am. Chem. Soc.*, 1989, **111**, 5542.
- 11 K. Murata, M. Aoki, T. Susuki, T. Harada, H. Kawabata, T. Komori, F. Ohseto, K. Ueda and S. Shinkai, *J. Am. Chem. Soc.*, 1994, **116**, 6664.
- 12 K. Hanabusa, K. Okui, K. Karaki, T. Koyama and H. Shirai, *J. Chem. Soc., Chem. Commun.*, 1992, 1371.
- 13 K. Hanabusa, M. Yamada, M. Kimura and H. Shirai, *Angew. Chem., Int. Ed. Engl.*, 1996, **35**, 1949.
- 14 P. Terech, C. Chachaty, J. Gaillard and A. M. Giroud-Godquin, *J. Phys. France*, 1987, **48**, 663.
- 15 S. Yamasaki and H. Tsutsumi, *Bull. Chem. Soc. Jpn.*, 1994, **67**, 906.
- 16 J. van Esch, S. De Feyter, R. M. Kellog, F. De Schryver and B. L. Feringa, *Chem. Eur. J.*, 1997, **3**, 1238.
- 17 N. Ide, T. Fukuda and T. Miyamoto, *Bull. Chem. Soc. Jpn.*, 1995, **68**, 3423.
- 18 L. Lu and R. G. Weiss, *J. Chem. Soc., Chem. Commun.*, 1996, 2029.
- 19 R. Mukkamala and R. G. Weiss, *J. Chem. Soc., Chem. Commun.*, 1995, 375.
- 20 E. W. Garbisch and D. B. Patterson, *J. Am. Chem. Soc.*, 1963, **85**, 3228.
- 21 G. D. Meakins, R. K. Percy, E. E. Richards and N. R. Young, *J. Chem. Soc. C*, 1968, 1106.
- 22 J. D. Ferry, in *Viscoelastic Properties of Polymers*, Wiley, New York, 1980.
- 23 K. Almdal, J. Dyre, S. Hvidt and O. Kramer, *Polymer Gels and Networks 1*, 1993, 5.
- 24 J. L. Jones and C. M. Marques, *J. Phys. France*, 1990, **51**, 1113.
- 25 K. Kon-no, T. Jin-no and A. Kitahara, *J. Colloid Interface Sci.*, 1974, **49**, 383.
- 26 F. Kaneko, O. Shirai, H. Miyamoto, M. Kobayashi and M. Suzuki, *J. Phys. Chem.*, 1994, **98**, 2185.
- 27 G. C. Pimentel and A. C. McClellan, in *The hydrogen bond*, Freeman, San Francisco, CA, 1960.
- 28 P. Terech, J. J. Allegraud and C. M. Garner, *Langmuir*, in press.
- 29 P. Terech, A. Coutin and A. M. Giroud, *J. Phys. Chem. B*, 1997, **101**, 6810.
- 30 T. Tachibana and H. Kamabara, *J. Colloid Interface Sci.*, 1968, **28**, 173.
- 31 J.-H. Fuhrhop, S. Svenson, C. Boettcher, E. Rössler and H.-M. Vieth, *J. Am. Chem. Soc.*, 1990, **112**, 4307.

Paper 8/01922C; Received 9th March, 1998